17th World Conference on Earthquake Engineering, 17WCEE
Sendai, Japan - September 13th to 18th 2020
Paper N° C002221
*Registration Code: S-**A02626***

NUMERICAL ANALYSIS AND EXPERIMENTAL CORRELATION OF UNCOUPLED CONCRETE WALLS INCORPORATING SLB DEVICES

M. Pantoja [1], M. Flores [2], L. Bozzo [3], H. Gonzales [4]

[1] *Structural engineer, Postensa SAC Lima-Peru, info.postensa@gmail.com*
[2] *MSc Structural engineer, Brunel University London-UK, 1739320@alumni.brunel.ac.uk*
[3] *Msc., PhD., General Director, Luis Bozzo Estructuras y Proyectos S.L. Barcelona-Spain, info@luisbozzo.com*
[4] *Msc., PhD., Structural engineer, Postensa SAC Lima-Peru, ing@postensa.pe*

Abstract

ACI 318-19 Code has substantially modified their ductility requirements for walls, resulting in an increment of cost and detailing. A different approach is to combine a bare reinforced concrete frame filled with concrete walls only connected to the frame at their base and their upper level by ductile connections such as SLBs. Since these devices do not transfer axial load, the solution is called "uncoupled" concrete walls. The combination of reinforced concrete frames and uncoupled walls with dissipators increases stiffness and ductility, but most importantly, allows the walls not to be aligned vertically, even in its full height, resulting in important architectural advantages. This work presents a comparison between an experimental and a numerical model of uncoupled reinforced concrete walls using Shear Link Bozzo (SLB) connections for a cyclic loading test performed at the UNAM laboratory in Mexico.

In order to understand the structural behavior of the SLB connections, three 1:1-scale tests were performed: (1) a bare reinforced concrete frame, (2) a reinforced concrete frame with 50kN SLB devices (Type 1) on uncoupled walls and (3) a reinforced concrete frame with 100kN SLB devices (Type 2) in the same uncoupled walls. These test results are used to validate numerical simulations of the system through Finite Element Analysis software; in this case, ABAQUS CAE. Once validated, the main parameters of the SLB connections are varied to understand how these affect the general behavior of the system. The purpose is to analyze the influence of the different parameters in the behavior of the SLB connections to propose alternatives to improve their performance.

For the bare reinforced concrete frame, the experimental force-displacement curve was quasi linear up to 14mm. For a similar level of lateral displacements incorporating SLB energy dissipators, a significantly stable nonlinear response with an initial yielding displacement of only 2mm was shown. After 14mm lateral displacement in test 2 and 3, type 1 and type 2 dissipators, reached lateral loads of 235kN and 320kN respectively. A significant measurement is that the hysteretic energy dissipation by types 1 and 2 devices was from 6 to 10 times greater than that of the bare reinforced concrete frame.

Analytical results showed that reducing the total height of the devices may contribute to dissipating more energy, despite failure displacement being proportionally reduced.

This means that a compact device could display a better performance using less material, which translates as a cheaper device, although it may not be feasible due to practical minimum lateral displacements requirements in codes. A model using horizontally fixed supports was implemented showing that it improves the behavior of the SLB connections, reaching up to 140% of the total load capacity of the system. Moreover, higher Von Mises stress distribution is displayed in the SLB connections, reaching high plastic deformations. However, the aforementioned theoretical improvements lost the "no vertical load transfer advantage" which is considered important for practical purposes.

Keywords: Shear Link Bozzo dissipators; experimental testing; dissipators; structural steel; uncoupled concrete walls.

1. Introduction

The SLB connections are characterized by their capacity to absorb high amount of energy and their relatively low cost [1,2]. These devices do not transfer axial load and connected to a concrete frame by means of a wall results in an isostatic system called, consequently, "uncoupled" wall. The combination of reinforced concrete frames and uncoupled walls with dissipators increases stiffness and ductility, but most importantly, allows the walls not to be aligned vertically, even in their full height or in the full beam length resulting in important architectural advantages. This work compares experimental and numerical model results for an uncoupled reinforced concrete wall using Shear Link Bozzo (SLB) connections for a cyclic loading test performed at the UNAM laboratory in Mexico (Figure 1).

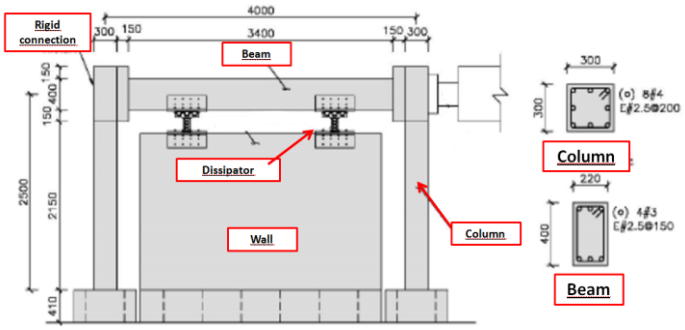

Fig. 1 – Dimensions of the reinforced concrete frame in mm [3]

In order to understand the structural behavior of the SLB connections and uncouple walls, three 1:1-scale tests were performed:

(1) A reinforced concrete frame without SLB connections.

(2) The same reinforced concrete frame using two SLB connections with a design capacity of 125 kN each on uncoupled walls

(3) The same reinforced concrete frame using two SLB connections with a design capacity of 250 kN each on uncoupled walls

The same loading pattern was used in the three tests which was controlled through displacements applied quasi statically.

The next task undertaken in this research is to correlate the results obtained by the experimental tests with numerical models which will represent the behavior of the structure under monotonic quasi static loads through the employment of finite element analysis software. ABAQUS CAE was chosen in order to simulate the test behavior. Once the numerical simulation is validated using the experimental results, varying several parameters such as the total height, dissipative height, width, thickness, position, dimension of the dissipators, and others will allow to study how each of these parameters can be modified to improve dissipative energy.

2. Test set up

2.1. SLB connections

SLB connections of two different capacities were used. The first is named "type 1", and it has an initial yielding strength of 125 KN each. The second one is named "type 2" and it has an initial yielding force of 250 KN each [3]. The main characteristic of the SLB device tested is the upper connection called "hair comb" or "Almena". These connections transfer only displacements significantly avoiding the transmission of axial load over the devices and, consequently, through the structural global configuration. The material of

the steel connections is, in general, structural steel ASTM A36, with a nominal strength of 250 MPa. Figure 2 shows dimensions of SLB connection type 1 and Fig. 3 for connection type 2.

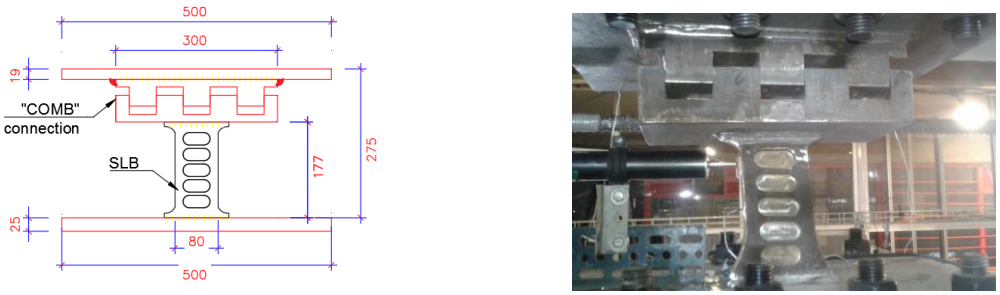

Fig. 2 – (a) Dimensions (mm) of SLB connection type 1 [1]. (b) SLB connection type 1[1].

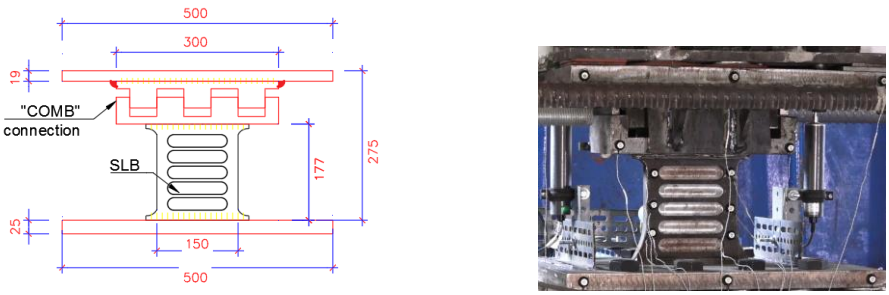

Fig. 3 – (a) Dimensions (mm) of SLB connection type 2. (b) SLB connection type 2

2.2. Concrete Frame

The reinforced concrete frame is composed of precast elements, which include: two columns of 30 x 30 cm, a beam of 22 x 40 cm and a shear wall of 15 cm of thickness. The beam is linked to the concrete columns through rigid bolted connections. The dimensions and steel reinforcement are shown in Fig. 4 [3]. It is important to emphasize that the concrete frame and the shear wall are not physically linked. The link between them is the SLB connections. Thus, when there are no SLB connections, the elements work separately. The SLB connections link the shear wall and concrete frame to create a frame – wall – SLB configuration system. As also shown in Fig. 4, the shear wall and columns were set over rigid foundations; the foundations were anchors applying a tension force of 200 kN which allowed to emulate fixed supports.

Fig. 4 – Reinforced concrete frame used in the test [3]

2.3.1. Loading pattern

Fig. 5 shows the test loading pattern. It consists of a history of displacements applied statically, with an actuator MTS with a capacity of ± 1000 KN and a maximum displacement of 200 mm. All the tests were controlled by displacements. The displacements were applied from 1 to 18 mm performing four loading cycles per each displacement level.

At the end of the test for SLB connection type 1, 20 cycles of 18 mm were applied in order to fatigue the SLB connection. For the connection type 2, some additional cycles were applied with higher deformation levels.

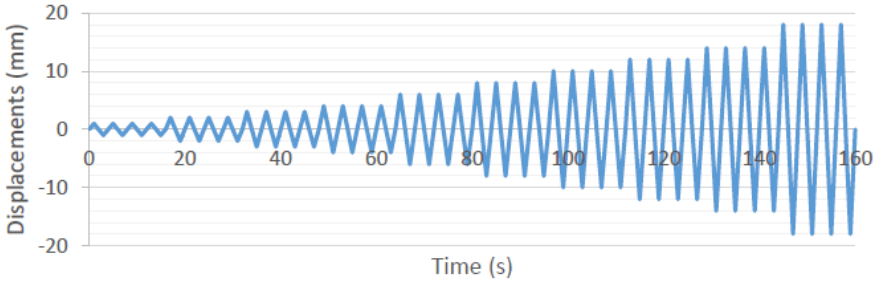

Fig. 5 – Pattern of applied displacements

3. Experimental results

Three tests were carried out under cyclic horizontal displacements of increasing amplitude in order to understand the behavior between concrete frame and SLB connections. The Fig. 6 shows a hysteresis curve and a *skeleton curve* (envelope of hysteresis curve) for the concrete frame without SLB connections.

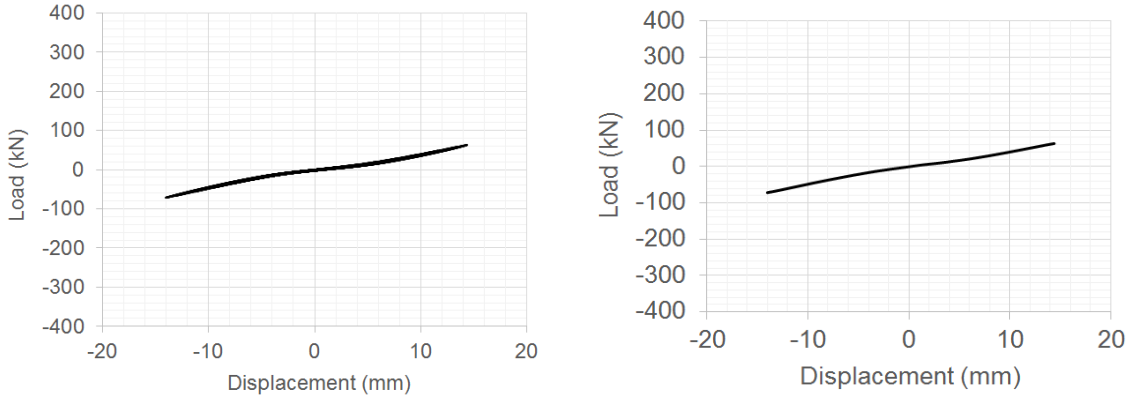

a) b)

Fig. 6 – Bare concrete frame a) Hysteresis curve, and (b) Skeleton curve [1]

According to Fig. 6, the frame without SLB connections exhibits an approximately linear elastic behavior without significant dissipated energy by concrete frame plasticity. The total lateral force applied, to achieve maximum positive lateral displacement of 14 mm, was 72 kN. Meanwhile, for achieving the maximum negative lateral displacement of 14.4 mm, it was 63.4 kN.

From the load-deformation hysteresis curve, the maximum drift ratio of the concrete frame is obtained as the ratio of the maximum lateral displacement and its height. This value (14.4/2500) was 0.576%, which is 18% lower than the maximum limit of Peruvian Seismic Code. The value of 0.7% is specified for concrete structures in E-030 code [4].

Figure 7 shows hysteresis and skeleton curves for the concrete frame with SLB connections type 1 through the un-coupled reinforced concrete wall. This figure shows that SLB connections type 1 exhibited a linear-elastic behavior up to achieving the yielding lateral displacement. The yielding load and displacement were approximately 100 kN and only 2 mm, respectively. After yielding, the values of lateral load and maximum displacement for positive branches of the hysteresis curve were of 234 kN and 15 mm. Meanwhile, for negative branches the obtained values were of 236 kN and 14.2 mm for lateral load and maximum displacement, respectively.

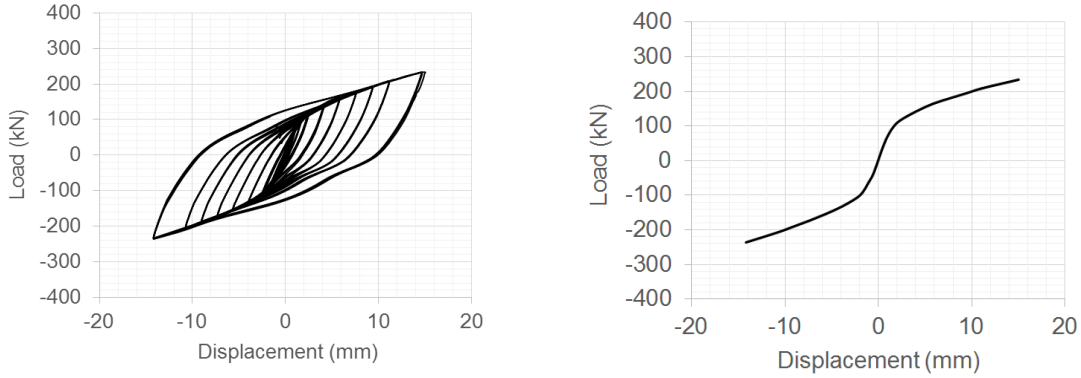

a) b)

Fig. 7 – Concrete frame with SLB connections type 1 a) Hysteresis curve, and (b) Skeleton curve [1].

The hysteresis curve shows that structural behavior of concrete frame with SLB connections type 1 exhibit steady hysteresis loops without loss of strength and stiffness degradation. As a result, SLB devices dissipate energy and the maximum drift ratio of the concrete frame with SLB connections type 1 was 15/2500 = 0.6%, which is also lower than the maximum limit of Peruvian Seismic Code [2] but for a significantly larger lateral force.

Figure 8 shows hysteresis and backbone curves for the concrete frame with SLB connections type 2 through decoupled reinforced concrete wall. This figure shows that SLB connections type 2 exhibited a linear-elastic behavior up to achieving the yielding lateral displacement. The yielding load and displacement were approximately of 130 kN and 2 mm, respectively. After yielding, the values of lateral load and maximum displacement for positive branches of the hysteresis curve were of 316 kN and 13.3 mm. Meanwhile, for negative branches the obtained values were of 325 kN and 12.7 mm for lateral load and maximum displacement, respectively.

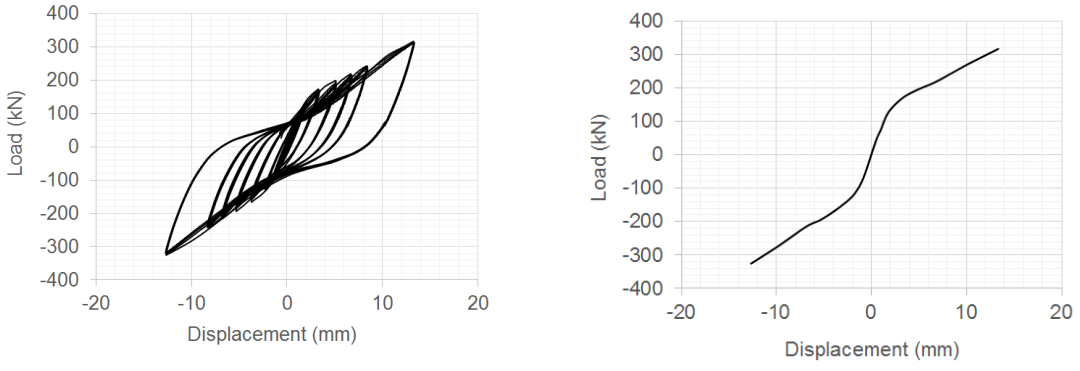

a) b)

Fig. 8 – Concrete frame with SLB connections type 2 a) Hysteresis curve, and (b) Skeleton curve [1].

The hysteresis curve shows an initial practically linear-elastic behavior but pinching of hysteresis curve appears as soon as relative displacements between connecting plates of the SLB connections and concrete shear wall occur. The origin of this "pinching of hysteresis curve" is that very important bolted connections of the devices (see Fig. 9) were unwittingly omitted in the laboratory

The hysteresis curve shows that structural behavior of concrete frame with SLB connections type 2 through decoupled reinforced concrete wall exhibit hysteresis loops without loss of strength, but some stiffness degradation. As a result, SLB devices dissipate energy and the maximum drift ratio of the concrete frame with SLB connections type 1 was 13.3/2500 = 0.532%, which is lower than the maximum limit of Peruvian Seismic Code [2].

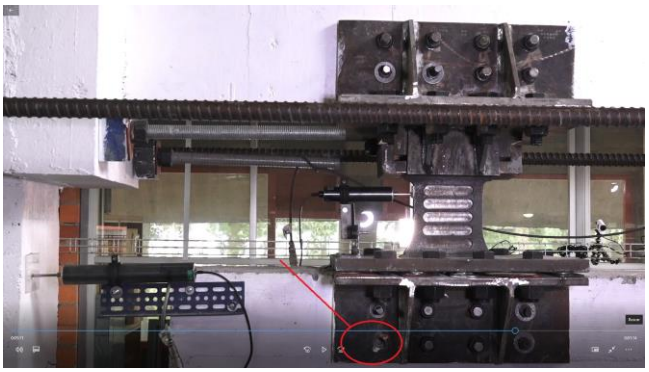

Fig. 9 – Unwittingly omitted important bolt not disposed in the tests

4. FEA modelling

The finite element analysis software ABAQUS CAE was used to simulate the experimental results of the tests through modeling, analysis, assembling, and visualization of structural components. In this article only the frame without SLB connections and the frame with SLB connections Type 1 are modelled since the frame with SLB connections Type 2 displayed an unexpected behavior (see fig. 9) due to the excessive displacements of the connecting plates according to the test recorded video [3]. Mesh configuration of FE model of the test is shown in Fig 10.

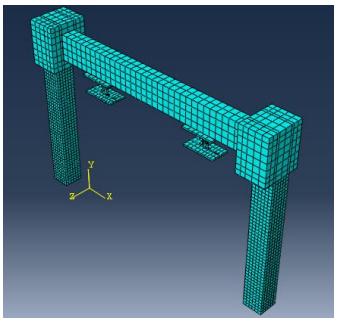

Fig. 10 – Mesh configuration of FE model of the test

4.1 Material properties

4.1.1 Constitutive model of reinforcing bar steel

Usually, the behaviour of the steel reinforcing bars is linear elastic at low strain demands. However, under high strain demands, it behaves inelastically, which implies plastic performance after reaching its yielding point. Before reaching its yielding point, deformation can be fully recovered if load is removed. Nonetheless, exceeding yield stresses will develop permanent deformations diminishing the stiffness of the section [5].

The yield strengths for longitudinal steel bars was considered as 420 MPa with Young's modulus of elasticity, Es = 200 GPa and Poisson's ratio, μ = 0.3.

4.1.2 Constitutive model of SLB connection steel

A tri-linear model is used, since the load pattern makes the structural steel in the SLB connections yield at minimum displacements and most of its behaviour displays plastic deformations. The material is a structural steel ASTM A36 with a nominal strength of Fy = 250 N/mm2 (see Fig. 11).

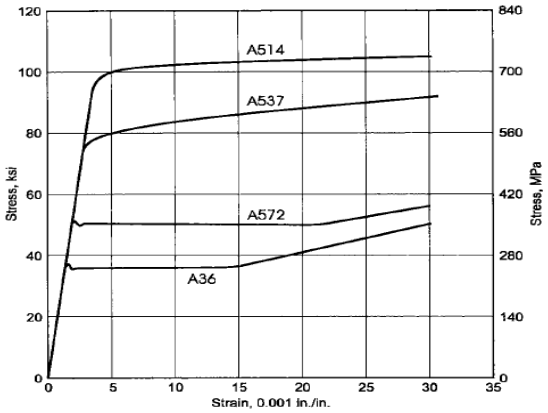

Fig. 11 – Tri-linear tress-strain curve for structural steel A36 [6].

4.1.3 Constitutive model of reinforced concrete

Linear at elastic and nonlinear damaged plasticity model for inelastic states of concrete are assumed because of concrete's low deformability in those both states. The concrete isotropic damage plasticity model is designed for its cyclic loading conditions. Degradation of the elastic stiffness induced by the plastic straining both in tension and compression are taken into consideration in the material constitutive model [7].

The concrete has been modelled using the constitutive model presented in Eurocode 2 for structural analysis. Young's Modulus of the concrete is 31926.07 N/mm2, the Poisson's Ratio value was assumed to be 0.2 and the crushing strength under compression is 34 N/mm2 according to sample tests under uniaxial compression.

4.2 Boundary conditions

According to the recorded video of the test (see http://luisbozzo.com/disipadores/), there were displacements and considerable rotations in the reaction wall due to (1) an unwittingly omitted important bolt and (2) lack of application of grout generating clearances between actual bolts and surrounding concrete. Consequently, the reaction wall on ABAQUS CAE model was not included. Alternatively, simpler, linear springs were used in order to simulate the response. In total 36 springs were used under the plates where the SLB connections were welded to the reaction wall with lineal stiffness as displayed in Table 1.

Table 1 – Spring Stiffness

Spring stiffness	
X – stiffness	350 N/mm
Z – stiffness	1000 N/mm

4.3 Mesh Sensitivity

In order to obtain good enough results through the use of the ABAQUS CAE software, the mode has been subjected to a number of analysis in order to see what elements affect most the behavior of the whole structure and how their mesh distributions affect the accuracy taking into account the computational effort. Therefore, the mesh used in this research is compared with finer ones in steel elements, and another using finer mesh in steel and concrete elements conveying very similar results with a small error of 0.6%. The used mesh distribution in this research project is applied due to its manageable computational time. Moreover, figure 13 shows that when using a finer mesh distribution in the steel elements next to the SLB connections, there is no appearance of Von Mises stresses which can be interpreted as an infinitive rigid behavior.

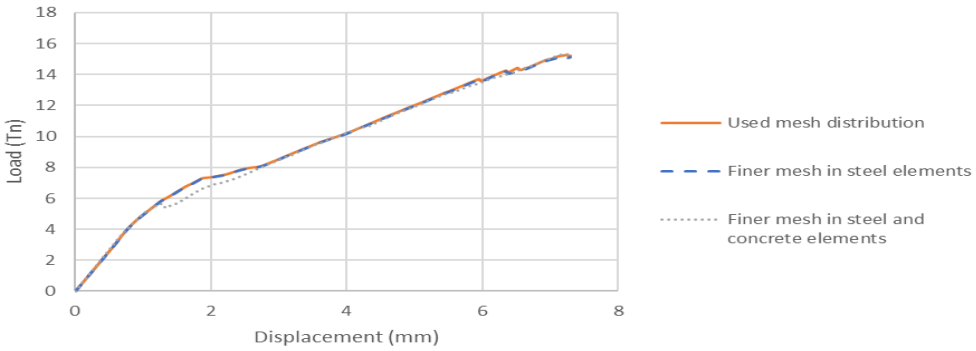

Fig. 12 – Load-Displacement relationship of "Concrete frame without SLB connections" (Experimental test – Numerical modelling)

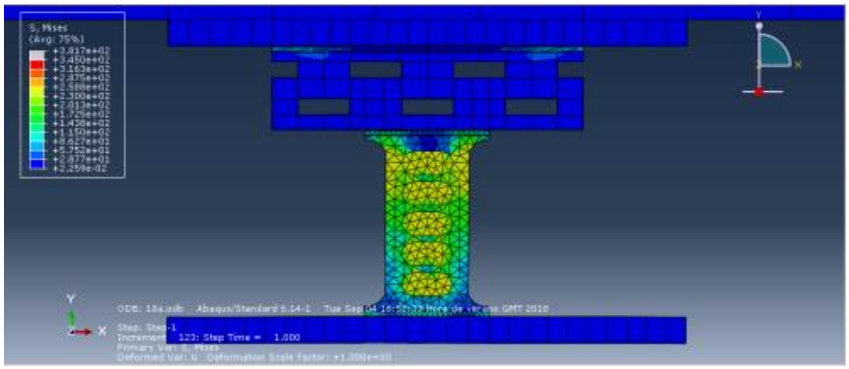

Figure 13-Von Mises tress distribution - finer mesh in steel elements

4.4 Validation

First the concrete frame without SLB connections was modeled in order to calibrate the model, and subsequently the uncoupled frame SLB connections type 1 was modeled until achieving the right behavior of the SLB connections.

4.4.1 Concrete frame without SLB connections

The first test executed was the "Uncoupled frame with SLB connections type 1"; during this test, the structure was subject to large displacements that provoked cracking at the base of the concrete columns. Therefore, the experimental response of the concrete frame without SLB connections behaved displaying stiffness of a cracked section as shown in Fig. 14.

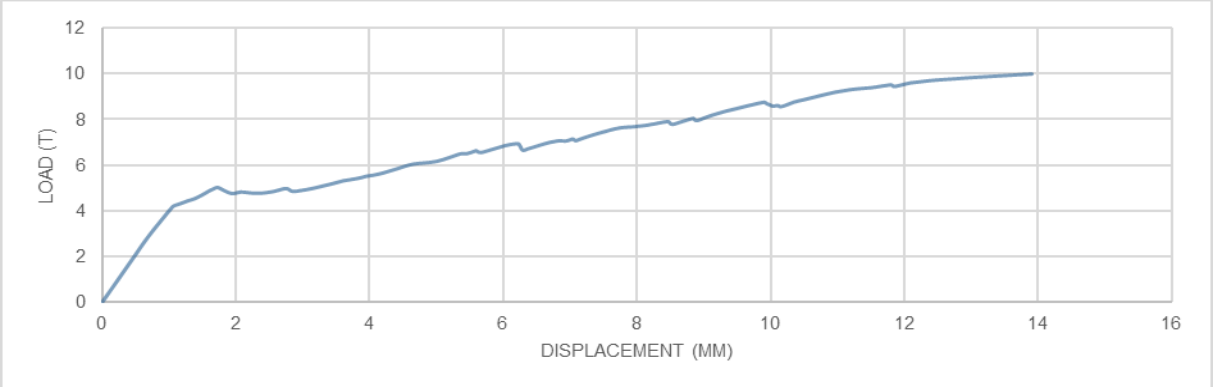

Fig. 14 – Load-Displacement relationship of "Concrete frame without SLB connections" (Experimental test)

Consequently, a complete cracked section was used in the numerical model. Drawing a trend line in both, the results of the experimental test and the cracked behavior of the numerical model, it can be seen in Fig. 15 that both results display a highly similar stiffness of 0.51 T/mm.

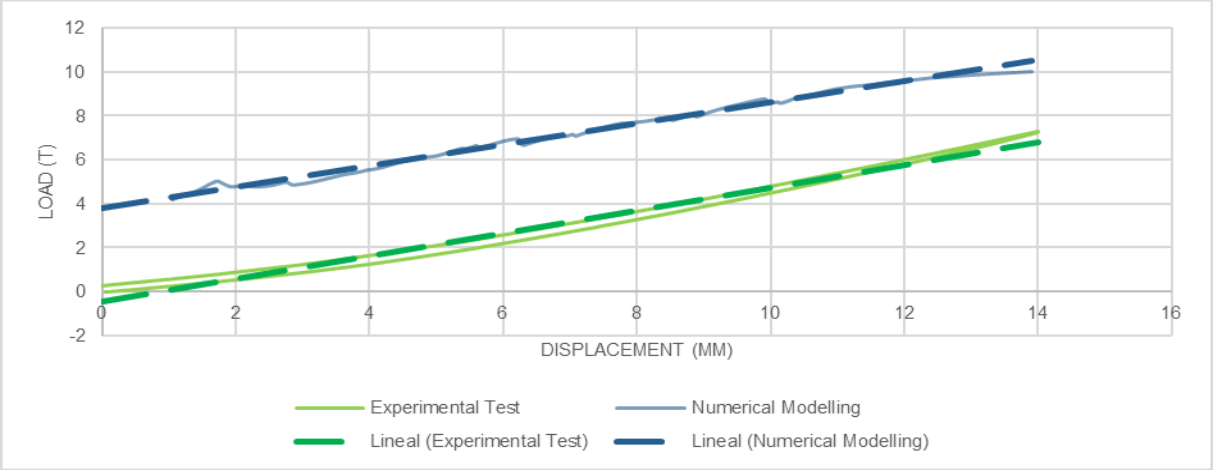

Fig. 15 – Load-Displacement relationship of "Concrete frame without SLB connections" (Experimental test – Numerical modelling)

4.4.2 Uncoupled frame with SLB connections type 1

Through several iterations to get the spring stiffness shown in Table 1, it was possible to obtain a numerical model that displays a similar behavior than the experimental test. Fig. 16 shows comparisons between experimental and numerical hysteresis loops.

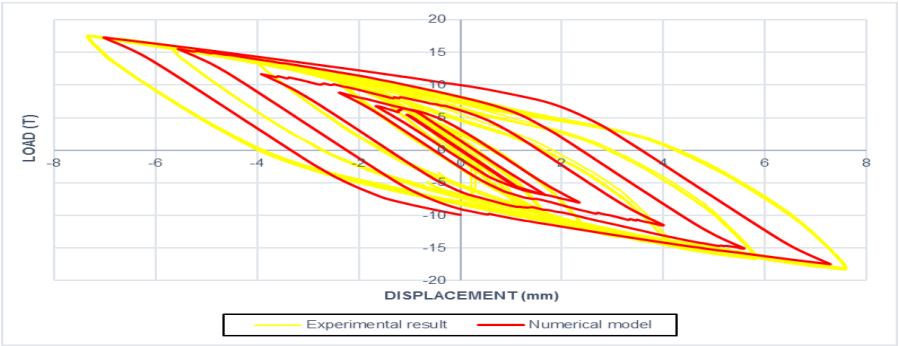

Fig. 16 – Comparison between experimental and numerical hysteresis loop of SLB connections type 1

As shown in Fig. 17, the stress distribution in the SLB connection type 1 is mainly distributed in the "windows" which are the thinner sections; however, the upper part of the frames also presents high stress levels. Furthermore, the welding sections are subject to minimum levels of stress. On the other hand, sections like steel plate and steel teeth (located over the SLB connection) do not display significant stress distribution.

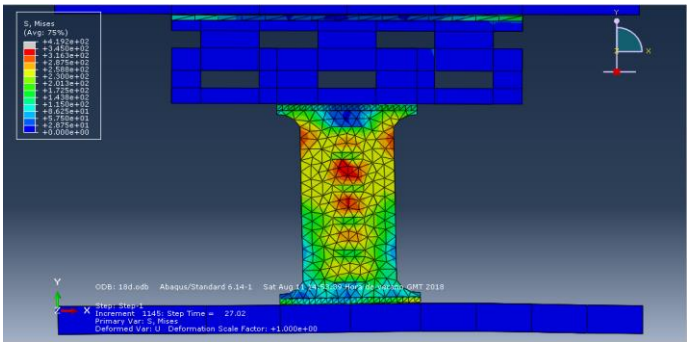

Fig. 17 – Von Misses stresses for the SLB connection Type 1

5. Influence of parameters

In order to understand which parameters of the test are the most relevant and how their geometry and position affect the results, parametric numerical analyses were done changing their dimensions as shown in Table 2.

Table 2 – Parameters variation

Parameters variation	
Total height	± 20 mm
Dissipative height	± 2 mm
Width	± 10 mm
Dissipative thickness	± 1 mm
Position	± 100 mm

5.1 Influence of Total height, dissipative height, width and dissipative thickness.

As displayed in Fig. 17, usually when increasing or diminishing the volume of the SLB connections, its load capacity improves or deteriorates respectively; however, increasing the height just worsen the whole performance of the SLB connections. It can be deducted that compact SLB connections have a better behavior although this highly depends on the level of maximum dissipative displacement. Taller devices are more flexible, and they would result in larger maximum or failure displacements which is directly related to maximum interstory drift codes. A maximum limit, such in Peruvian code of 0,007 for a 320 interstory height results in a maximum device demand of 22mm while a drift limit of 0,01 would demand 32mm. Consequently, the maximum capacity of the device is directly related to the maximum displacement demand in the specific local code. Certainly, larger failure displacement demands result in more expensive larger devices.

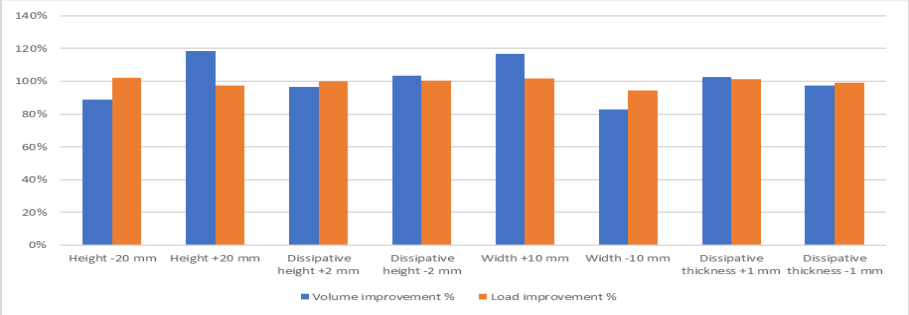

Fig. 17 – Influence of different parameters – numerical models (%)

5.2 Influence of Position

The horizontal distance between the SLB connections is 2300 mm, however, it is a concern how much distance between them will allow achieving a better performance, therefore, several numerical tests were carried out using different horizontal distances.

As shown in Fig. 18, the behavior of the SLB connections can be improved by varying its horizontal distance along the reaction wall. However, the betterment in behavior is negligible due to low values.

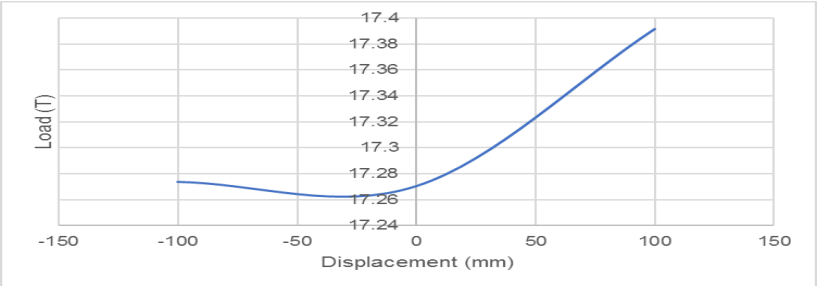

Fig. 18 – Influence of position – numerical models

5.3 Fixed supports

A model using fixed supports was implemented as shown in Fig. 19 and it shows that using good connections between the reaction wall and the SLB devices, the behavior of the SLB connections is improved significantly, reaching values of 140% of the load capacity of the model using spring supports. Consequently, the connection of this stiff devices is a significant parameter for future studies, although it is also clear that the actual experimental test connections were very poor due to the aforementioned two facts (see 4.2).

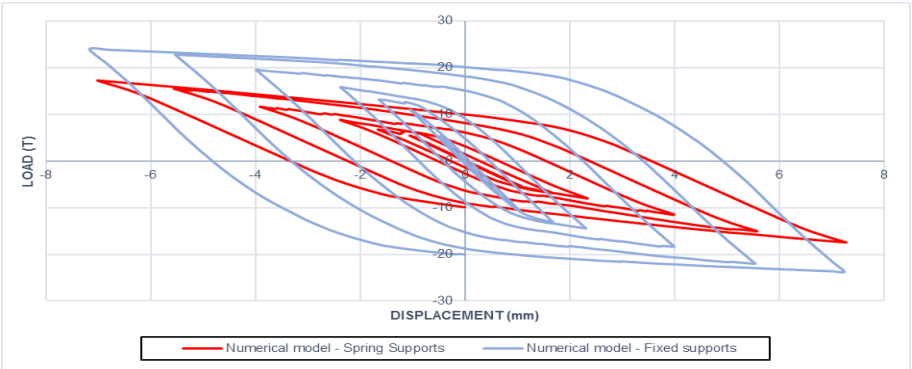

Fig. 19 – Comparison between spring supports and fixed supports numerical model

6. Conclusions

The nonlinear FE models displayed good numerical correlation with experimental results, conveying well-shaped hysteretic curves. The test sequence significantly influenced the numerical validation due to the fact that the concrete columns were already cracked when the second test started. Consequently, cracked concrete stiffness for the frame was used for the model. Furthermore, the modeling of the uncoupled walls had to be replaced by linear springs at the SLBs bottom base plates since there was not a good anchorage connection at the laboratory specimen. Specifically, there was one anchorage fully missing, as well as no concrete grout at the anchorage rod holes which originates cyclic flattening. The free space around the horizontal anchorage rods and the tolerance required for installation generated a negative impact causing local concrete crushing under the applied cyclic loading. As a consequence, a correct construction of the laboratory specimen model would have provided even better final results in terms of dissipative energy and maximum failure displacement.

It is observed that increasing the height of the SLB devices worsens its behavior. However, while reducing the total height of the device, the SLB devices reaches higher plasticity demands. This implies that a compact device can display a better performance using less material resulting in a cheaper dissipator but maximum breaking point displacement may be not enough for local code provisions or double height braces or walls supporting these devices.

It is observed that the right position of the SLB devices within the uncoupled wall has a minimum impact on overall results. According to the tests, while distancing the devices from each other, their performances reach higher moments values; however, changing their position provides a minimum improvement or degradation and consequently it is not the most influential parameter.

Finally, using fixed supports instead of spring ones for the devices, dissipates more energy, being an effective way to improve the behavior of the structure. Fixed supports physically mean that complete displacement and rotation restrictions are assumed at the SLBs extremes. In order to achieve this in the test, the connection between the bottom plate of the device and the uncoupled wall should work without slipping or relevant movements. The drawback of fixed supports is that “no axial force transfer” advantage would be lost and the devices could not be freely installed in plan and elevation.

7. References

[1] Bozzo L, Barbat AH (1999): *Diseño sismorresistente de edificios. Técnicas convencionales y avanzadas.* Editorial Reverte. Barcelona, Spain

[2] Bozzo L, et al. (2019), *Modeling, Analysis and Seismic Design of Structures Using Energy Dissipators SLB.* Journal TECNIA Vol.29 N°2 July-December 2019, Lima, Peru.

[3] Instituto de Ingenieria UNAM (2017): Experimental test of a reinforced concrete frame equiped with seismic energy dissipators "SLB". Ciudad de Mexico: Universidad Nacional Autónoma de México. (in Spanish)

[4] E.030 (2018): Building Technical Code. Earthquake-resistant design. Ministry of housing, construction and sewage. Lima, Peru (in Spanish).

[5] Ahmed, A. (2014) 'Modeling of a reinforced concrete beam subjected to impact vibration using ABAQUS'. International journal of civil and structural engineering, 4(3), pp. 227-236

[6] ASM International (2002): Atlas of Stress-Strain Curves. 2nd edn. United States of America: The Materials Information Society.

[7] Dassault Systèmes Simulia Corp. (2010) Abaqus Analysis User's Manual. Available at: https://www.sharcnet.ca/Software/Abaqus610/Documentation/docs/v6.10/books/usb/default.htm?startat=pt05ch20s06abm38.html (Accessed: 08 August 2018).